Original Article

Institution of MECHANICAL ENGINEERS
Journal of AUTOMOBILE ENGINEERING

Proc IMechE Part D:
J Automobile Engineering
1–13

DOI: 10.1177/0954407014547243
pid.sagepub.com
SAGE

A model-based rear-end collision avoidance algorithm for heavy commercial road vehicles

Vignesh Rajaram and Shankar C Subramanian

Abstract

A rear-end collision is one of the most frequent accidents occurring on roadways. In this paper, a model-based longitudinal collision avoidance algorithm is developed for heavy commercial road vehicles to avoid rear-end collisions. This paper focuses on the inclusion of the dynamics of the pneumatic brake system in the collision avoidance algorithm. The developed algorithm also considers the dynamic behaviour of the heavy vehicle during braking such as the dynamic load transfer, the dynamic brake force distribution between the wheels and the maximum traction available at the tyre–road interface. The pressure transients in the brake chamber are modelled as a linear first-order dynamic system with a time delay. Commercially available vehicle dynamic simulation software, TruckSim, is used for simulating the developed control algorithm for realistic traffic scenarios with different loading and road conditions. The results obtained from the simulations are compared with the experimental results obtained from a hardware-in-the-loop system and the simulation results are found to be promising.

Keywords

Collision avoidance, heavy commercial vehicles, rear-end collision, pneumatic brake system, vehicle dynamics, active safety, longitudinal control

Date received: 13 February 2014; accepted: 21 July 2014

Introduction

In spite of the advancements in automobile technology and road infrastructure, the number of road accidents keeps increasing every year.[1] Research conducted by the National Highway Traffic Safety Administration (NHTSA) shows that one third of fatalities in road vehicle traffic crashes were speed related.[2] In India, heavy vehicles such as buses and trucks account for less than 6% of the total registered vehicles[3] but, according to the statistics provided by the National Crime Records Bureau, heavy vehicles are responsible for 28.6% of total road accident fatalities in the year 2012.[1] When compared with other road vehicles, the per vehicle fatalities for heavy trucks are much higher.[4] A rear-end collision is one of the common causes of heavy-vehicle accidents. In fact, 345,000 crashes involving large trucks and buses were reported in the USA during the year 2011,[5] of which 21.7% of crashes were due to rear-end collisions. A rear-end collision is an accident in which a vehicle crashes into a vehicle travelling in front of it. These accidents arise mostly because the driver misjudges the speed of the vehicle in front, does not maintain a safe distance from the vehicle in front and is inattentive.[2,6] Longitudinal driving assistance systems such as adaptive cruise control, stop-and-go control and collision avoidance systems (CASs) can assist drivers in preventing such accidents. A CAS helps the driver to avoid accidents by continuously monitoring the area in front of the vehicle with the help of radar and/or cameras. If the CAS detects a vehicle, it measures the distance and the relative velocity between the vehicles, and the control algorithm evaluates the threat level. In the event of a potential collision, the CAS alerts the driver and, if the driver fails to react or the brake force provided by the driver is not sufficient to avoid the collision, then the CAS takes

Department of Engineering Design, Indian Institute of Technology Madras, Chennai, Tamil Nadu, India

Corresponding author:
Shankar C Subramanian, Department of Engineering Design, Indian Institute of Technology Madras, Chennai, Tamil Nadu 600036, India.
Email: shankarram@iitm.ac.in

control of the brake system and applies the brake automatically to avoid the collision.

A few collision warning and collision avoidance algorithms[7–11] were developed on the basis of the kinematics of the vehicles. Jansson et al.[12] proposed a method to compute the risk for collision by considering the measurement uncertainties and driver manoeuvres. Yi et al.[13] proposed a sliding-mode controller for a collision warning and collision avoidance algorithm used in passenger cars. Recently, researchers developed a collision detection system[14] and a CAS[15] considering the vehicle dynamics and the brake dynamics for passenger cars. The focus of the existing literature on CASs is mainly on passenger cars, where the prime importance is given to safety, and the cost of introducing the advanced safety systems is a secondary factor. Vehicle manufacturers such as Volvo, Ford, Honda and General Motors have already introduced collision warning and collision avoidance systems in their high-end passenger cars.[16] Minami et al.[17] and Hirano[18] developed a collision warning system for heavy vehicles based on the kinematic details. In these algorithms, vehicle dynamics and brake dynamics have not been given much importance. Vehicle dynamics and brake dynamics in heavy vehicles are different from those in passenger cars. In passenger cars, the laden weight and the unladen weight do not vary significantly. However, in the case of heavy vehicles, the laden vehicle weight and the unladen vehicle weight vary to a greater extent. Therefore, it is important to develop a control algorithm for heavy commercial road vehicles considering the dynamics of the vehicle. The brake system used in heavy vehicles is also different from that used in passenger cars. The brake system in heavy vehicles is typically designed for the fully loaded condition and hence, during unloaded conditions, there is a possibility of excessive braking, which may result in tyre lock. The pneumatic brake system used in conventional heavy vehicles also has a significant time lag and slower response, and recent research has focused on addressing this issue. Miller and co-workers[19,20] proposed a high-speed binary actuated valve to speed up the response of the brake system of a heavy vehicle. Karthikeyan et al.[21] proposed an electro-pneumatic brake (EPB) system to reduce the time lag and developed a mathematical model for the EPB system. The EPB system also facilitates the integration of anti-lock brake system and traction control system functionalities. Mahanty and Subramanian[22] developed a slip controller for an EPB system in heavy commercial vehicles. Suh et al.[23] developed a mathematical model of the tractor–semitrailer and the air brake system including an anti-lock brake system. The literature related to a CAS using the EPB system for heavy commercial vehicles is not currently available. Moreover, constrained by the economic factors in countries such as India, heavy-vehicle owners are not required to install costly driver assistance devices in their vehicles. The drivers are constrained to drive for a longer time[24] to increase their throughput, leading to fatigue and accidents. In order to address these problems, it is important to develop a cost-effective safety system for heavy vehicles, which assists the driver in ensuring safe operation. Considering these factors, a control algorithm for a CAS including the vehicle dynamics and the brake system dynamics was developed in this paper. It is expected that the CAS that will be developed in the long term can be integrated in an existing heavy commercial vehicle with minimal hardware changes.

In this paper, the control algorithm for the CAS is developed for heavy vehicles with an EPB system. The vehicle model considered for braking analysis includes aerodynamic drag, rolling resistance, road grade and tyre–road interaction. The dynamic phenomena of heavy vehicles such as the load transfer during braking and the brake force distribution between the wheels are also considered. A linear first-order model with a time delay for the brake chamber pressure transients is used to characterize the overall braking performance of the heavy vehicle. The proposed collision avoidance algorithm predicts a collision based on a distance and a relative velocity between the host vehicle (a vehicle in which the CAS is fitted) and the lead vehicle (a vehicle that is travelling in front of the host vehicle). The developed control algorithm is tested for various realistic traffic scenarios using commercially available vehicle dynamic simulation software (TruckSim) and the results are compared with the experimental data obtained from hardware-in-the-loop (HIL) testing.

Vehicle model

Longitudinal vehicle model during braking. The resisting forces acting on a two-axle heavy commercial road vehicle together with the braking forces are shown in Figure 1. The forces acting are the aerodynamic resistance R_a, the rolling resistance R_{rf} of each of the front tyres, the rolling resistance R_{rr} of each of the rear tyres, the grade resistance R_g, the braking force F_{bf} developed at each of the front tyres and the braking force F_{br} developed at each of each of the rear tyres. The equation of motion along the longitudinal direction of the vehicle moving on a straight road is given by

$$Ma = -R_a - 2R_{rf} - 2R_{rr} - R_g - 2F_{br} - 2F_{bf}$$

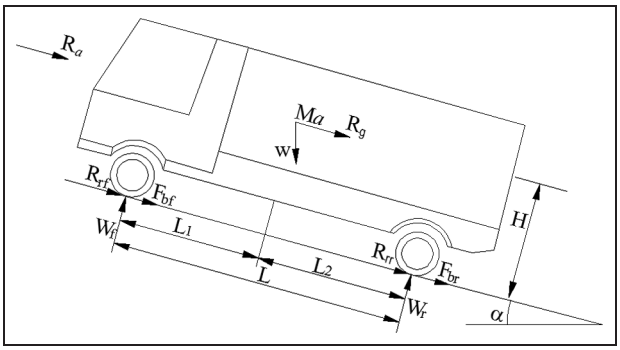

Figure 1. Longitudinal dynamics of the vehicle during braking.

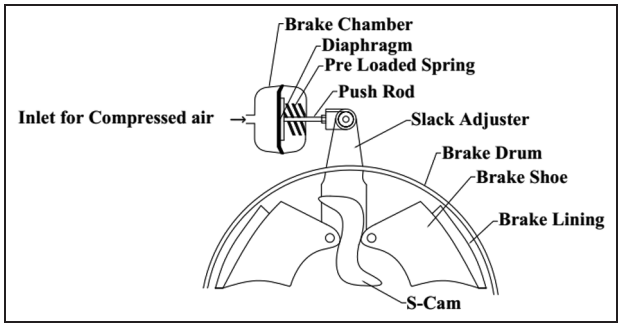

Figure 2. S-cam foundation brake.

where M is the mass of the vehicle and a is the acceleration of the vehicle (for deceleration, a is taken as negative). This can be rewritten as

$$Ma = -R_a - R_r - R_g - F_b \tag{1}$$

where $R_r = 2R_{rf} + 2R_{rr}$ and $F_b = 2F_{br} + 2F_{bf}$.

The aerodynamic resistance is expressed as $R_a = \rho a_f c_d v^2/2$, where ρ is the density of air, a_f is the frontal area of the vehicle, c_d is the aerodynamic drag coefficient and v is the velocity of the vehicle.

The rolling resistance is taken as $R_r = f_r W \cos(\alpha)$ where W is the weight of the vehicle, f_r is the coefficient of rolling resistance[25] ($f_r = 0.006 + 0.23\times10^6 v^2$) and α is the grade angle. The grade resistance is given by $R_g = W \sin(\alpha)$.

Brake system in heavy vehicles. In this paper, S-cam drum brakes, commonly used as foundation brakes in heavy commercial vehicles, are considered. The typical S-cam foundation brake is illustrated in Figure 2.

The pneumatic brake system used in heavy commercial vehicles consists mainly of a pressure source, pressure regulation and brake actuation. The compressor is the pressure source, which sends the compressed air to the pressure regulation device based on the driver's pedal force; the pressure regulation device meters the compressed air to the brake chamber and generates a force to push the push rod. The push rod rotates the S-cam through the slack adjuster. The rotation of the S-cam forces the brake shoe to come into contact with the brake drum, which results in vehicle deceleration. When the brake pedal is released, the air from the brake chamber is exhausted through the exhaust port. Because of the presence of the return spring, the contact between the brake shoe and the brake drum is released.

Brake force calculation. A relation between the braking torque and the brake chamber pressure has been given by Limpert.[26] It is modified to include the brake chamber contact pressure, and the braking force is given by

$$F_{brake} = \frac{\eta(p_b - p_{co}) a_b l_{sa} r_d \text{ BF}}{2 r_t r_c} \tag{2}$$

where η is the efficiency of the brake system, p_b is the pressure in the brake chamber, p_{co} is the contact pressure (the pressure at the which the brake shoe comes into contact with the brake drum), a_b is the area of the brake chamber, l_{sa} is the length of the slack adjuster, r_t is the radius of the tyre, r_d is the inner radius of the brake drum, r_c is the effective radius of the S-cam and BF is the brake factor. The BF is defined as the ratio of the braking force generated on the brake drum to the actuation force on the corresponding brake shoe. It depends on the brake dimensions and the coefficient of friction between the brake pad and the brake drum.

From equation (2), it is evident that the brake force is proportional to the effective brake chamber pressure $(p_b - p_{co})$ and the brake chamber area a_b. Considering two brakes per axle, the braking force developed at each of the front wheels and the braking force developed at each of the rear wheels are given by

$$F_{fbrake} = (p_b - p_{co}) a_{b_f} C_b \tag{3a}$$

and

$$F_{rbrake} = (p_b - p_{co}) a_{b_r} C_b \tag{3b}$$

respectively, where $C_b = (\eta l_{sa} r_d \text{ BF})/2 r_t r_c$, a_{b_f} is the area of the front brake chamber and a_{b_r} is the area of the rear brake chamber.

The load distribution plays an important role in determination of the braking performance in heavy vehicles, because it determines the braking effort that can be supported at each wheel. The load distribution between the front wheels and the rear wheels varies during braking owing to the dynamic load transfer from the rear wheels to the front wheels. In this paper, it was assumed that the vehicle is travelling on a straight flat road, and hence the vertical load acting on the left wheels and the vertical load acting on the right wheels of the vehicle were assumed to be the same and invariant. The load on each of the front wheels and the load on each of the rear wheels are given by

$$W_f = \frac{1}{2L}\left[WL_2 + H\left(-Ma - R_a - R_g\right)\right] \tag{4a}$$

and

$$W_r = \frac{1}{2L}\left[WL_1 - H\left(-Ma - R_a - R_g\right)\right] \tag{4b}$$

respectively where L is the length of the wheelbase, H is the height of the vehicle's centre of gravity (CG) from the ground level, L_1 is the distance from the vehicle's CG to the front axle and L_2 is the distance from the vehicle's CG to the rear axle.

The maximum braking force developed on the vehicle is limited by two factors:

(a) the maximum traction that the tyre–road interface can support, which depends on the normal load and the coefficient of tyre–road adhesion;

(b) the maximum braking ability of the vehicle's brake system, which depends on the maximum supply pressure, the brake chamber area, the length of the slack adjuster, the radius of the S-cam and the dimensions of the brake components.

The maximum force that the tyre–road contact can support is given by

$$F_{bmax} = \mu W$$

where μ is the coefficient of adhesion at the tyre–road interface.

For a two-axle vehicle, the maximum braking force on each of the front wheels and the maximum braking force on each of the rear wheels are given by

$$F_{bfmax} = \mu W_f \tag{5a}$$

and

$$F_{brmax} = \mu W_r \tag{5b}$$

respectively.

When the braking force generated by the brake system at a wheel is greater than the above value, then that wheel locks. This kind of situation arises, for example, when the vehicle is unladen and the driver applies full braking or during brake application on road surfaces with a lower coefficient of adhesion, which leads to loss of vehicle control and/or steerability.

The maximum braking force on the vehicle is developed only when the distribution of the braking force between the wheels is exactly in the same proportions as that of the normal load on the wheels. This braking force distribution between the front wheels and the rear wheels is given by

$$\frac{K_{bf}}{K_{br}} = \frac{F_{bfmax}}{F_{brmax}} \tag{6}$$

where K_{bf} and K_{br} are the proportion of the total braking force on the front wheels and the proportion of the total braking force on the rear wheels respectively. Thus,

$$K_{bf} + K_{br} = 1 \tag{7}$$

From equations (6) and (7), the values of K_{bf} and K_{br} were computed. The values of K_{bf} and K_{br} were calculated at each iteration on the basis of the corresponding updated values of W_f and W_r calculated using equation (4). It should be noted from equation (4) that the values of W_f and W_r at any instant of time depend on the deceleration at that particular instant of time.

From equations (3) and (5) the maximum braking force generated at each of the front tyre–road interfaces and the maximum braking force generated at each of the rear tyre–road interfaces at any instant are given by

$$F_{bf} = \min\left(F_{f_{brake}}, F_{bfmax}\right)$$

and

$$F_{br} = \min(F_{r_{brake}}, F_{brmax})$$

respectively.

Mathematical model for the brake chamber pressure transients

In the conventional brake system used in heavy commercial road vehicles, the compressed air is supplied to the mechanically operated treadle valve and then to relay valves. When the driver presses the brake pedal mounted on the treadle valve, the exhaust ports of the treadle valve are closed and then the inlet ports are opened to meter out the compressed air to the brake chamber. This results in a significant time delay (the time interval elapsed between the input given to the brake actuator and the time at which the pressure starts to increase in the brake chamber), which results in a slower response of the brake system. A detailed description and layout of the conventional pneumatic brake system used in heavy vehicles can be found in the literature.[27] The steady-state relation between the treadle valve plunger displacement and the pressure transients in the brake chamber has also been found to be nonlinear.[27]

In order to introduce the CAS in heavy vehicles, it is important to have an EPB system that is more suitable for automatic control. The EPB system uses electronically operated values, which reduces the brake time delay τ and improves the brake system response time (the time taken by the brake system to reach the steady-state pressure in the brake chamber from the instant of its application). The brake time delay and the brake response time are important parameters in deciding the stopping distance. Thus, an EPB system helps to reduce the stopping distance and thereby can potentially help to avoid accidents or to mitigate an accident's severity. In this paper, an EPB system with an electro-pneumatic regulator (EPR) is considered. When the driver presses the brake pedal, an electric signal is given to the EPR, which is the brake actuator in the EPB system, and it supplies compressed air to the brake chamber corresponding to the input voltage signal. It has been experimentally found that the steady-state brake chamber pressure is proportional to the input voltage signal given to the EPR.[21] The relationship is given by

$$p_{bss}(t) = a_2 V_{reg} + p_{atm} \tag{8}$$

where a_2 is a constant and V_{reg} is the input voltage to the EPR.

For the purpose of developing the collision avoidance algorithm, the brake chamber pressure transients in the EPB system are modelled as a linear first-order dynamic system with a time delay.[28] The governing equation for the brake chamber pressure is given by

$$a_1 \dot{\tilde{p}}_b(t) + \tilde{p}_b(t) = a_2 u(t - \tau)$$

where a_1 and a_2 are constants that can be experimentally determined, $\tilde{p}_b(t)$ is the brake chamber gauge pressure, given by $\tilde{p}_b(t) = p_b(t) - p_{atm}$, and $u(t-\tau)$ is the voltage input to the EPR with τ being the time delay in the system that has been experimentally determined as 30 ms for step inputs. The input to the brake actuator (the EPR) by the CAS can be approximated as a step input, since the brake is automatically applied only in emergency conditions.

The open-loop system transfer function is given by

$$G(s) = \frac{\tilde{p}_b(s)}{U(s)} = \frac{a_2}{1 + a_1 s} e^{-\tau s}$$

The time delay term $e^{-\tau s}$ is approximated using the Padé first-order approximation, which is given by $(2 - \tau s)/(2 + \tau s)$.

In order to regulate the desired brake chamber pressure required by the CAS, a proportional–integral–derivative (PID) controller with the transfer function $H(s)$ is developed, and the closed-loop transfer function is given by

$$\frac{\tilde{p}_{b,act}}{\tilde{p}_{b,des}} = \frac{H(s)G(s)}{1 + H(s)G(s)} \tag{9}$$

where $\tilde{p}_{b,act}$ and $\tilde{p}_{b,des}$ are the actual brake chamber pressure and the desired brake chamber pressure respectively.

Controller design for CAS

The main objective of a CAS is to prevent a collision by automatically applying brakes in the case of a potential collision. The distance and the relative velocity between the host vehicle and the lead vehicle are used to assess the safe situation of the host vehicle. In order to achieve this objective, the relative velocity $v_r(t)$ and the distance $x_r(t)$ between the vehicles have to be regulated. The relative velocity is given by

$$v_r(t) = v_l(t) - v_h(t)$$

where $v_l(t)$ and $v_h(t)$ are the velocity of the lead vehicle and the velocity of the host vehicle respectively. The safe or desired distance (the minimum distance that a host vehicle has to maintain from a lead vehicle to avoid accidents when both the vehicles are travelling with the same velocity) between the vehicles is given by

$$s_d(t) = hv_h(t) + s_o$$

where h is the headway time (the time elapsed between the front of the lead vehicle passing a point on a roadway to the time at which the front of the host vehicle passing the same point considering the prevailing velocity of the host vehicle) and s_o is the headway offset (the minimum headway distance when the host vehicle stops against the preceding vehicle). The value of h can be modified on the basis of various parameters such as the mass of the vehicle, the maximum braking capacity of the vehicle, the driver's response time, the brake system's response time, the available coefficient of tyre–road adhesion and the type of lead vehicle. Considering the driver's reaction time[29] as 1.25 s, the value h is taken as 1.25 s for a laden vehicle and 1.10 s for an unladen vehicle in this paper. The headway offset distance s_o is usually taken as the length of the lead vehicle[30] and is taken as 10 m.

The actual distance between the lead vehicle and the host vehicle is measured using radar, and the difference between the measured distance $x_r(t)$ and the desired distance $s_d(t)$ is given by

$$\delta(t) = x_r(t) - s_d(t) \tag{10}$$

where $x_r(t) = x_l(t) - x_h(t)$ and $x_l(t)$ and $x_h(t)$ are the position of the lead vehicle and the position of the host vehicle respectively at the time instant t.

Ioannou and Zu[31] proposed a throttle and brake controller for automatic vehicle following. Their brake control design was based on the assumption that the braking torque developed is proportional to the brake line pressure while ignoring the dynamics of the brake system. In this paper, the algorithm was developed for EPBs, and a similar approach was followed for calculating the required brake force, but while considering the brake system dynamics. This is important since the response time of the EPB is sufficiently significant for its dynamics to be explicitly included in the design process.

The relevant vehicle dynamic variables are given by the equations

$$\begin{aligned} v_r(t) &= v_l(t) - v_h(t) \\ \delta(t) &= x_r(t) - hv_h(t) - s_o \end{aligned} \tag{11}$$

The acceleration of the host vehicle is obtained from equation (1) as

$$a_h(t) = -\frac{1}{M}\left(F_b + R_a + R_r + R_g\right) \tag{12}$$

Substituting $a_h(t) = u(t)$, where $u(t) = -(F_b + R_a + R_r + R_g)/M$ and the control input $u(t)$ is chosen in such a way that it stabilizes the system given by equation (11) as

$$u(t) = k_1 v_r(t) + k_2 \delta(t) \tag{13}$$

where k_1 and k_2 are constants. Substituting equation (13) in equation (12) and using $a_h(t) = \dot{v}_h(t)$, equation (12) is transformed to

$$\dot{v}_h(t) = k_1 v_r(t) + k_2 \delta(t) \tag{14}$$

From equations (11) and (14), taking $v_r(t)$ and $\delta(t)$ as the state variables and using the Laplace transform give

$$\begin{aligned} v_r(s) &= \frac{(s + k_2 h)s}{\Delta(s)} v_l + \frac{k_2 s}{\Delta(s)} s_o \\ \delta(s) &= \frac{(1 - k_1 h)s}{\Delta(s)} v_l - \frac{(s + k_2)s}{\Delta(s)} s_o \end{aligned} \tag{15}$$

where $\Delta(s) = s^2 + (k_1 + k_2 h)s + k_2$.

From equation (15), the stability of the system is assured, if $k_1 > -k_2 h$ and $k_2 > 0$. By choosing $k_1 = 1/h, \delta \to 0$ as $t \to \infty$ and in order to achieve a fast response without any overshoot in v_r, the denominator polynomial $\Delta(s)$ is equated to that of a critically damped second-order system and the value of k_2 is calculated as $1/h^2$.

The braking force required to achieve the desired acceleration is given by

$$F_b = \begin{cases} 0, & \text{if } -M(k_1 v_r + k_2\delta) < R_a + R_r + R_g \\ -\left[M(k_1 v_r + k_2\delta) + R_a + R_r + R_g\right], & \text{otherwise} \end{cases} \quad (16)$$

Considering the brake force distribution between the wheels given by equation (6), the brake force F_{bfreq} required from each of the front wheels and the brake force F_{brreq} required from each of the rear wheels are calculated as

$$F_{bfreq} = \frac{K_{bf} F_b}{2} \quad (17a)$$

and

$$F_{brreq} = \frac{K_{br} F_b}{2} \quad (17b)$$

respectively.

Considering the fact that the maximum braking force generated at the tyre–road interface is restricted by equation (5), the braking force generated from each of the front wheels and the braking force generated from each of the rear wheels are given by

$$F_{bf} = \min\left(F_{bfreq}, F_{bf\max}\right) \quad (18a)$$

and

$$F_{br} = \min\left(F_{brreq}, F_{brmax}\right) \quad (18b)$$

respectively.

The total braking force developed by a vehicle is given by

$$F_b = 2F_{bf} + 2F_{br}$$

In the S-cam air brake system, the braking force starts to develop only when the brake shoe is pressed against the rotating brake drum. In order for the brake shoe to press against the brake drum, the force produced from the brake chamber has to overcome the spring pre-load in the brake chamber. Including the spring pre-load, the braking force F_{bcf} required from each of the front brake chambers and the braking force F_{bcr} required from each of the rear brake chambers to achieve the desired deceleration are given by

$$F_{bcf} = \frac{F_{bf}}{C_b} + F_{fpl} \quad (19a)$$

and

$$F_{bcr} = \frac{F_{br}}{C_b} + F_{rpl} \quad (19b)$$

where F_{fpl} and F_{rpl} are the spring pre-load in the front brake chamber and the spring pre-load in the rear brake chamber respectively.

The brake chamber pressure required to develop the required front brake chamber force and the brake chamber pressure required to develop the required rear brake chamber force are given by

$$p_{b_f} = \frac{F_{bcf}}{a_{b_f}} \quad (20a)$$

and

$$p_{b_r} = \frac{F_{bcr}}{a_{b_r}} \quad (20b)$$

respectively.

Simulations and experimental results

The pressure in the brake chamber depends on the input voltage to the EPR and it is calculated using equations (8) and (20). The experimental set-up of the HIL test system is illustrated in Figure 3. It consists of a front axle and a rear axle with brake chambers. A pressure sensor is mounted at the inlet of each brake chamber and the pressure input to the brake chamber

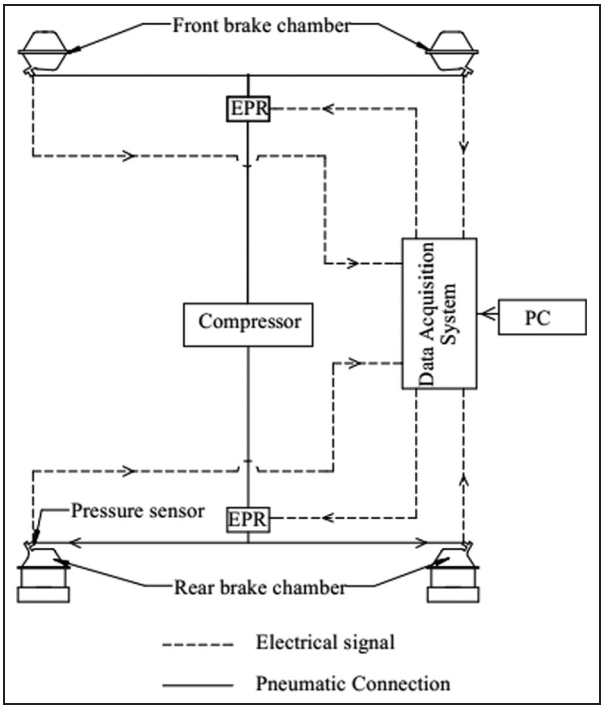

Figure 3. A schematic representation of the experimental set-up.
EPR: electro-pneumatic regulator; PC: personal computer.

Table 1. Values calculated from the experiment.

Parameter	Value
a_1	1.0 s
a_2	90,000 Pa/V
F_{fpl}	322 N
F_{rpl}	322 N

is regulated by the EPR. The experiments are carried out with the two EPR configuration. One EPR regulates the pressure to the two front brake chambers, and another EPR regulates the pressure to the two rear brake chambers. The parameter values related to the brake subsystem are found from experiments carried out on the set-up available and are listed in Table 1.

The desired brake chamber pressure was physically realized on the experimental set-up. In this regard, a PID controller is designed and it is used in the closed-loop transfer function of the EPR control algorithm given by equation (9) for regulating the pressure transients in the brake chamber. The EPR control algorithm helps to reduce the difference between the actual chamber pressure and the desired brake chamber pressure. Hence, the EPR control algorithm is a part of the collision avoidance algorithm. The actual brake chamber pressure (which includes the brake system dynamics) is provided to the collision avoidance algorithm so that it can factor in the EPR response and the brake system response. This coupled the collision avoidance algorithm and the EPR control algorithm. The range of values for the controller gains are obtained using the Routh stability criteria. The values of the controller gains are tuned from the simulation results. These values are the proportional gain $k_p = 5.6660 \times 10^{-5}$ V/Pa, the integral gain $k_i = 1.0034 \times 10^{-5}$ V/Pa s and the derivative gain $k_d = 0.0018 \times 10^{-5}$ V s/Pa.

The simulations and HIL implementation were carried out for three scenarios that are likely to be encountered in high-speed traffic on Indian highways,[32,33] especially during the night. It is known that these accidents are caused mainly by a high speed and driver fatigue. The scenarios are as follows (Figure 4).

1. *Lead vehicle at rest*. A host vehicle, travelling at a constant speed, encounters a stopped lead vehicle. This scenario happens on highways during nighttime or adverse weather conditions. If the driver is not sufficiently quick to react to the situation, then a collision may happen.
2. *Vehicle following*. A host vehicle and a lead vehicle are travelling at a constant speed by maintaining a safe distance between them. Then the lead vehicle suddenly starts to decelerate at a constant rate. If the driver of the host vehicle is inattentive or underestimates the threat level, there is a chance of an accident.
3. *Lane change*. A vehicle travelling in an adjacent lane enters into the path of the host vehicle and becomes the lead vehicle; it then starts to decelerate at a constant rate. This is a typical lane-change scenario in multi-lane highways.

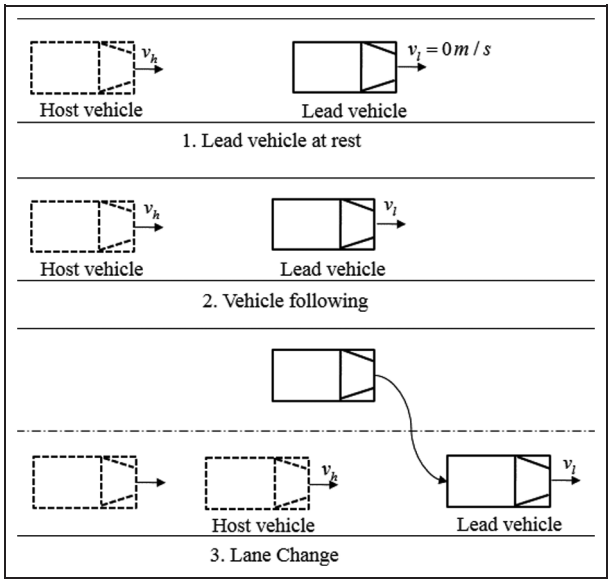

Figure 4. Representation of the traffic scenarios.

In all the scenarios described above, the CAS helps to detect a potential collision and stops the host vehicle within a safe distance constrained by the headway offset.

The algorithm was simulated for high-speed traffic scenarios with a road adhesion coefficient $\mu = 0.8$ corresponding to a dry-road condition and for low-speed scenarios with a road adhesion coefficient $\mu = 0.35$ corresponding to a wet-road condition for laden and unladen conditions.

The vehicle dynamic model presented before is used for the simulations, and the required brake chamber pressure is calculated on the basis of the relative velocity and the distance. The required brake chamber pressure is given as the input to TruckSim, and the deceleration $\dot{v}_h$ of the host vehicle is obtained as the output. The brake chamber pressure is controlled using the closed-loop system. TruckSim software is used in order to make the dynamic analysis of the vehicle more realistic.

In the case of HIL testing, the required brake chamber pressure obtained from the simulations is realized in the experimental set-up by providing the corresponding voltage to the EPR. The deceleration of the vehicle is calculated from the brake chamber pressure measured using the pressure sensor. The results obtained from the TruckSim simulations and the HIL testing were compared.

The parameters used for the simulations are listed in Tables 2 and 3. The values of the vehicle parameters are those for the Ashok Leyland Hawk 160 midibus.[34] The results obtained from the TruckSim simulations and the HIL testing are listed in Tables 4 and 5 for a laden vehicle and in Tables 6 and 7 for an unladen vehicle.

Table 2. Brake parameters used in the simulations.

Parameter	Value
l_{sa}	0.160 m
r_c	0.0127 m
r_d	0.194 m
a_{b_f}	0.0129 m^2
a_{b_r}	0.0155 m^2
BF	1.42
η	0.7
p_{max}	800 kPa

BF: brake factor.

Table 3. Parameters used in the simulations.

Parameter	Value	
	Laden	Unladen
W_f (static)	37,965 N	27,566 N
W_r (static)	69,945 N	14, 813 N
H	1.0 m	0.8 m
L_1	2.722 m	1.168 m
L	4.2 m	
ρ	1.2 kg/m^3	
r_t	0.480 m	

In Tables 4–7, the term 'Initial distance' refers to the distance between the lead vehicle and the host vehicle, when the CAS takes control of the vehicle's brake system. The term 'Final distance' refers to the final distance between the lead vehicle and the host vehicle when both the vehicles have come to rest. In the case of a lane-change scenario, 'Final distance' refers to the distance between the host vehicle and the vehicle that enters into the host vehicle's lane from the adjacent lane. The acceleration of the lead vehicle and its values are taken considering the worst-case scenario for the given road condition. The acceleration of the lead vehicle is taken as $-8\,m/s^2$ for $\mu = 0.8$ and $-3\,m/s^2$ for $\mu = 0.35$. In order to make the testing scenarios more realistic, higher speed values are used for $\mu = 0.8$ and lower speed values for $\mu = 0.35$. From the above results, it can be observed that the proposed algorithm is able to stop the host vehicle within a safe distance constrained by the headway offset ($s_o = 10\,m$).

The TruckSim simulations and the HIL results for the vehicle-following scenario for a laden vehicle and an unladen vehicle are shown in Figure 5 and Figure 6 respectively. The host vehicle and the lead vehicle are moving at the same speed of 25 m/s (90 km/h) by maintaining a safe distance. The lead vehicle suddenly starts

Table 4. Results for a laden vehicle with $\mu = 0.8$ and $h = 1.25$ s.

Scenario	Host-vehicle velocity v_h (m/s)	Lead-vehicle velocity v_l (m/s)	Lead-vehicle acceleration a_l (m/s^2)	Initial distance (m)	Final distance (m)	
					TruckSim	HIL
1	25	0	—	72.5	9.99	10.15
2	25	25	–8	41.25	9.99	10.16
3	25	20	–8	42	9.99	9.80

HIL: hardware-in-the-loop.

Table 5. Results for a laden vehicle with $\mu = 0.35$ and $h = 1.25$ s.

Scenario	Host-vehicle velocity v_h (m/s)	Lead-vehicle velocity v_l (m/s)	Lead-vehicle acceleration a_l (m/s^2)	Initial distance (m)	Final distance (m)	
					TruckSim	HIL
1	10	0	—	35	9.90	10.14
2	10	10	–3	22.5	9.98	10.14
3	10	8	–3	20	10.1	10.15

HIL: hardware-in-the-loop.

Table 6. Results for an unladen vehicle with $\mu = 0.8$ and $h = 1.1$ s.

Scenario	Host-vehicle velocity v_h (m/s)	Lead-vehicle velocity v_l (m/s)	Lead-vehicle acceleration a_l (m/s^2)	Initial distance (m)	Final distance (m)	
					TruckSim	HIL
1	25	0	—	65	9.81	10.04
2	25	25	–8	37.5	9.81	10.07
3	25	20	–8	42	9.81	9.97

HIL: hardware-in-the-loop.

Table 7. Results for an unladen vehicle with $\mu = 0.35$ and $h = 1.1$ s.

Scenario	Host-vehicle velocity v_h (m/s)	Lead-vehicle velocity v_l (m/s)	Lead-vehicle acceleration a_l (m/s^2)	Initial distance (m)	Final distance (m)	
					TruckSim	HIL
1	10	0	—	32	9.77	10.08
2	10	10	–3	21	9.77	10.08
3	10	8	–3	20	9.78	10.10

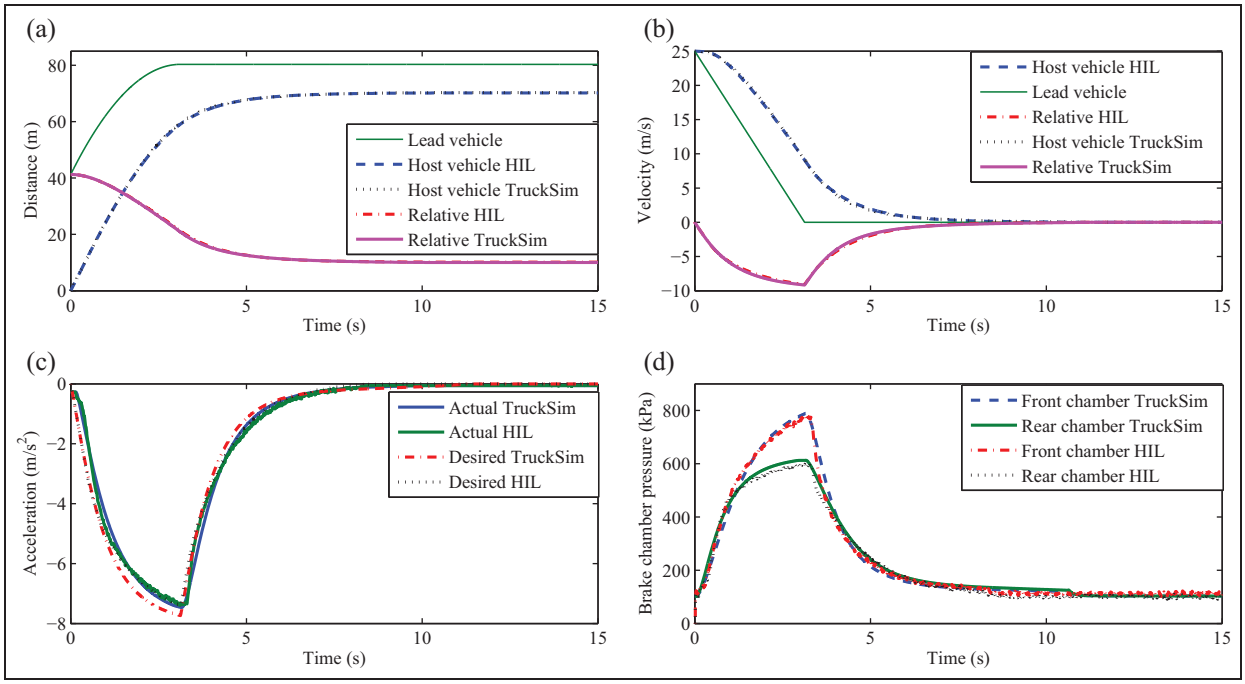

Figure 5. Vehicle-following scenario with $\mu = 0.8$ and $h = 1.25$ s for a laden vehicle: (a) position; (b) velocity; (c) acceleration; (d) brake chamber pressure.
HIL: hardware-in-the-loop.

to decelerate at a constant rate ($8\ m/s^2$). Therefore, the relative velocity between the vehicles increases and the distance between the vehicle decreases. The initial distance between the vehicles is selected in such a way that the desired distance and the actual distance are the same. The CAS predicts the collision and activates the brake actuator as soon as the lead vehicle starts to decelerate. From Figure 5(c) and Figure 6(c), it can be observed that the desired deceleration required by the vehicle is able to follow the actual profile to maintain a safe distance and a safe velocity, since the required braking force is less than the maximum braking capacity. This can be observed from the corresponding pressure profiles in Figure 5(d) and Figure 6(d).

In the case of the lead vehicle in the at-rest scenario for a laden vehicle, the deceleration required is high in order to maintain a safe distance and a safe velocity. However, the braking force developed at the front wheels is restricted by the maximum operating air pressure in the host vehicle. It can be seen from Figure 7(d) that the front brake chamber pressure becomes saturated once it reaches about 800 kPa (the maximum supply pressure). The braking capacity of the rear wheels is restricted by the maximum force that the tyre–road interface can support and hence the actual deceleration of the host vehicle (Figure 7(c)) is less than the desired deceleration.

For the case of the lane-change scenario in an unladen vehicle, in order to prevent wheel locking, the maximum braking force developed at each of the front wheels and the maximum braking force developed at each of the rear wheels are restricted by the maximum force that the tyre–road interface can support, which can be seen from the brake chamber pressure profile (Figure 8(d)). Hence, the actual deceleration of the host vehicle is limited (Figure 8(c)).

From these results, it is observed that the proposed collision avoidance algorithm is able to prevent the accident by maintaining a safe distance and a safe velocity for the given road conditions.

Conclusion

When compared with the existing collision avoidance algorithms (the Mazda algorithm,[7] the Berkeley algorithm[8] and the NHTSA algorithm[9]) based on the

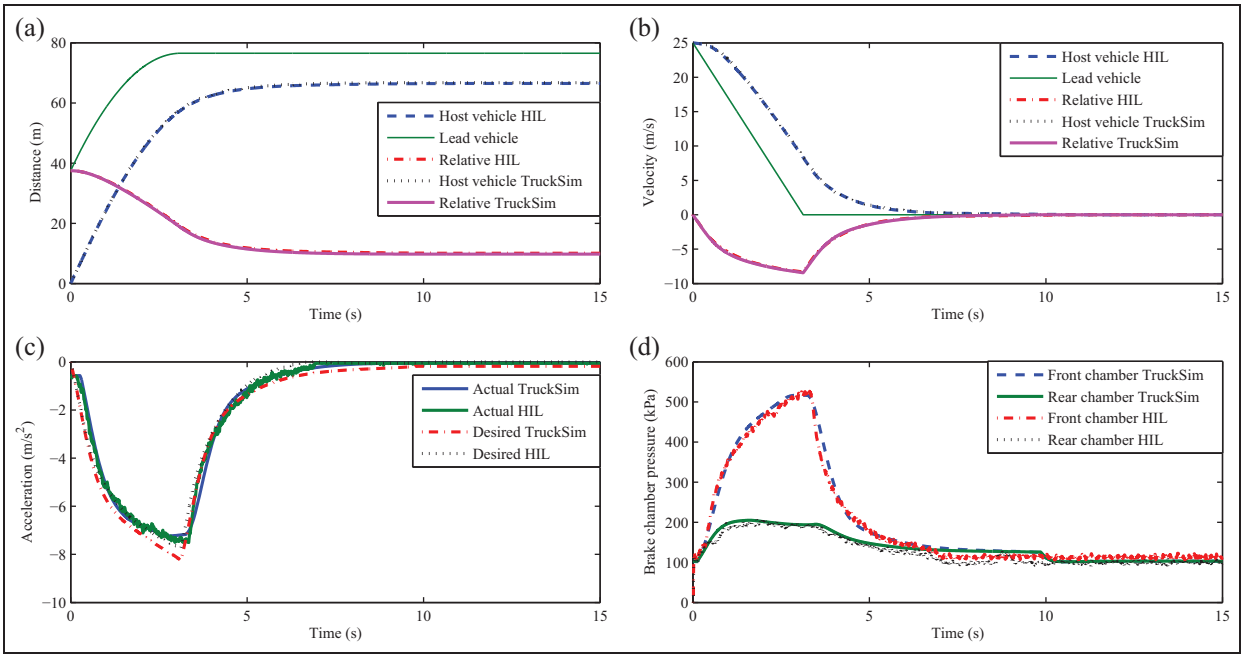

Figure 6. Vehicle-following scenario with $\mu = 0.8$ and $h = 1.1$ s for an unladen vehicle: (a) position; (b) velocity; (c) acceleration; (d) brake chamber pressure.
HIL: hardware-in-the-loop.

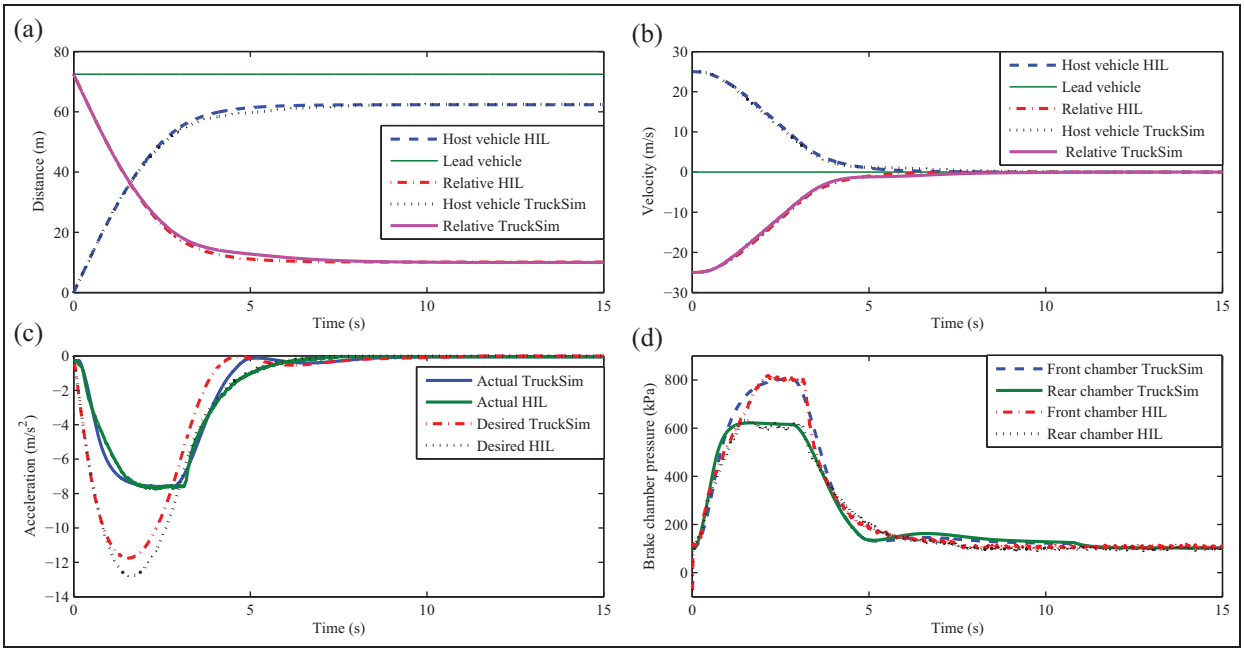

Figure 7. Lead vehicle in the at-rest scenario with $\mu = 0.8$ and $h = 1.25$ s for a laden vehicle: (a) position; (b) velocity; (c) acceleration; (d) brake chamber pressure.
HIL: hardware-in-the-loop.

kinematics of the vehicle, the proposed algorithm in this paper is more realistic, since it includes the vehicle dynamics and the brake system dynamics of the heavy commercial vehicle. The developed algorithm was evaluated using vehicle dynamic simulation software (TruckSim) and the HIL experimental system for three different scenarios corresponding to Indian highway traffic with different road and load conditions. The experimental results show that the proposed algorithm was able to prevent the collision and to stop the vehicle within a safe distance. The proposed algorithm would be helpful to implement a collision avoidance system in a heavy commercial vehicle with an EPB system.

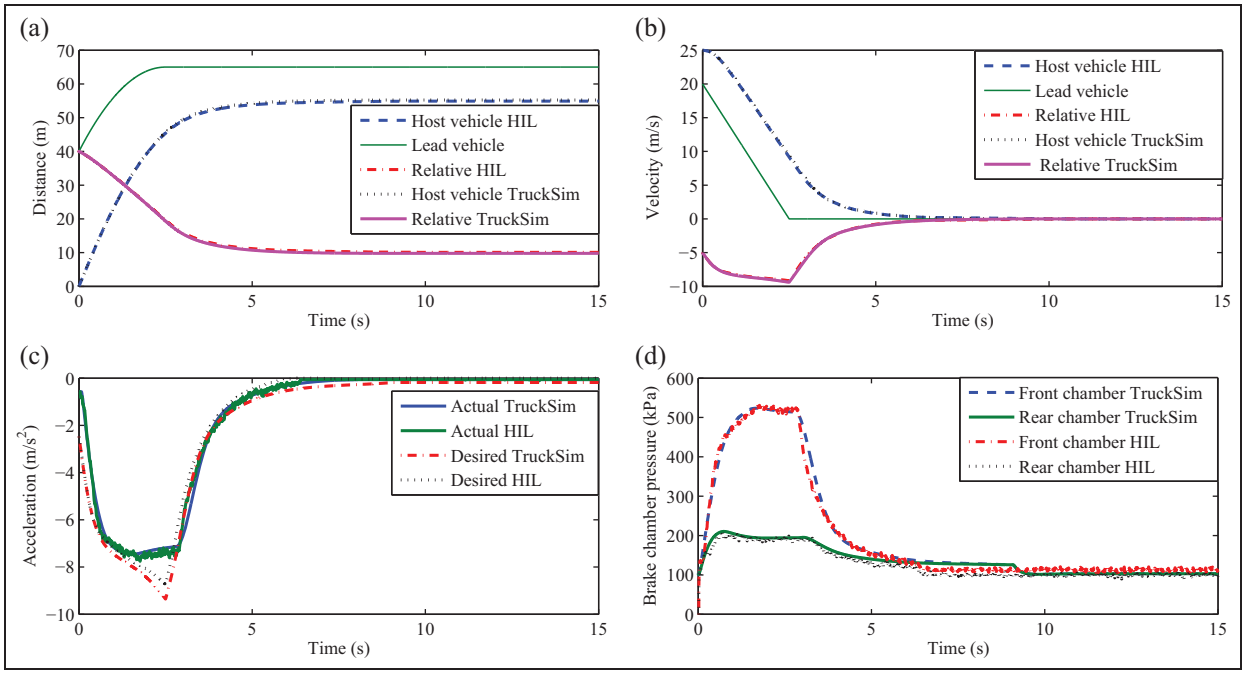

Figure 8. Lane-change scenario with $\mu = 0.8$ and $h = 1.1$ s for an unladen vehicle: (a) position; (b) velocity; (c) acceleration; (d) brake chamber pressure.
HIL: hardware-in-the-loop.

Declaration of conflict of interest

The authors declare that there is no conflict of interest.

Funding

This research received no specific grant from any funding agency in the public, commercial or not-for-profit sectors.

References

1. Accidental deaths and suicides in India 2012. Report, National Crime Records Bureau, Ministry of Home Affairs, Government of India, New Delhi, India, 2012.
2. Analysis of speeding-related fatal motor vehicle traffic crashes. Technical Report DOT HS 809 839, National Highway Traffic Safety Administration, US Department of Transportation, Washington, DC, USA, June 2005.
3. *Road transport year book (2011–2012)*. New Delhi: Transport Research Wing, Ministry of Road Transport and Highways, Government of India, 2013.
4. Mayhew DR, Simpson HM and Beirness DJ. Heavy trucks and road crashes. Report, Traffic Injury Research Foundation, Ottawa, March 2004.
5. Traffic safety facts 2011. Report DOT HS 811 754, National Highway Traffic Safety Administration, US Department of Transportation, Washington DC, USA, 2011.
6. Dagan E, Mano O, Stein GP and Shashua A. Forward collision warning with a single camera. In: *IEEE intelligent vehicles symposium*, Parma, Italy, 14–17 June 2004, pp. 37–42. New York: IEEE.
7. Doi A, Butsuen T, Niibe T et al. Development of a rear-end collision avoidance system with automatic brake control. *JSAE Rev* 1994; 15: 335–340.
8. Seiler P, Song B and Hedrick JK. Development of a collision avoidance system. SAE paper 980853, 1998.
9. Brunson SJ, Kyle EM, Phamdo N and Preziotti G. Alert algorithm development program NHTSA rear-end collision alert algorithm. Final Report DOT HS 809 526, National Highway Traffic Safety Administration, US Department of Transportation, Washington DC, USA, September 2002.
10. Moon S, Moon I and Yi K. Design, tuning, and evaluation of a full-range adaptive cruise control system with collision avoidance. *Control Engng Practice* 2009; 17(4): 442–455.
11. Sun ZL, Wang XK and Zai S-X. Research on collision avoidance method of car anti-head-and-rear based on safe distance model. *Advd Mater Res* 2011; 243–249: 4435–4440.
12. Jansson J, Johansson J and Gustafsson F. Decision making for collision avoidance systems. SAE paper 2002-01-0403, 2002.
13. Yi K, Woo M, Kim SH and Lee SC. An experimental investigation of a CW/CA system for automobiles using hardware-in-the-loop simulations. In: *American control conference*, San Diego, California, USA, 1999, pp.724–728. New York: IEEE.
14. Lee D, Han K and Huh K. Collision detection system design using a multi-layer laser scanner for collision mitigation. *Proc IMechE Part D: J Automobile Engineering* 2012; 226(7): 905–914.
15. Su JL and Ordys AW. Collision avoidance manoeuvre for a vehicle – a practical approach. *Proc IMechE Part D: J Automobile Engineering* 2010; 224(3): 299–312.
16. Palermo N. 6 Affordable vehicles with collision warning systems, http://www.autotrader.com/research/article/best-cars/188920/6-affordable-vehicles-with-collision-warning-systems.jsp (2014; accessed May 2014).

17. Minami K, Yasuma T, Okabayashi S et al. A collision-avoidance warning system using laser radar. SAE paper 881859, 1988.
18. Hirano M. Development of vehicle-following distance warning system for trucks and buses. In: *IEEE conference on vehicle navigation and information systems*, Ottawa, Canada, 12–15 October 1993; pp.513–516. New York: IEEE.
19. Miller JI and Cebon D. Modelling and performance of a pneumatic brake actuator. *Proc IMechE Part C: J Mechanical Engineering Science* 2011; 226(8): 2077–2092.
20. Miller JI, Henderson LM and Cebon D. Designing and testing an advanced pneumatic braking system for heavy vehicles. *Proc IMechE Part C: J Mechanical Engineering Science* 2011; 227(8):1715–1729.
21. Karthikeyan P, Siva Chaitanya C, Jagga Raju N and Subramanian SC. Modelling an electropneumatic brake system for commercial vehicles. *IET Electr Systems Transpn* 2011; 1(1): 41–48.
22. Mahanty S and Subramanian SC. A non-linear model-based slip controller for electropneumatic brakes in heavy commercial vehicles. *Int J Heavy Veh Systems* 2013; 20(1): 35–60.
23. Suh MW, Park YK and Kwon SJ. Braking performance simulation for a tractor–semitrailer vehicle with an air brake system. *Proc IMechE Part D: J Automobile Engineering* 2002; 216(1): 43–54.
24. Debroy B and Kaushik PD. A background paper on barriers to inter-state trade and commerce – the case of road transport. Report, Ministry of Law and Justice, National Commission to Review the Working of the Constitution, http://lawmin.nic.in/ncrwc/finalreport/v2b3–5.htm (2002, accessed May 2014).
25. Wong JY. *Theory of ground vehicles*. 3rd edition. New York: John Wiley, 2001, p.17.
26. Limpert R. *Brake design and safety*. 2nd edition. Warrendale, Pennslyvania: SAE International, 1991, p. 278.
27. Subramanian SC. *A diagnostic system for air brakes in commercial vehicles*. PhD Thesis, Texas A & M University, College Station, Texas, USA, 2006.
28. Kumar YSRR, Sonawane DB and Subramanian SC. Application of PID control to an electro-pneumatic brake system. *Int J Adv Engng Sci Appl Math* 2012; 4(4): 260–268.
29. Zhang Y, Antonsson EK and Grote K. A new threat assessment measure for collision avoidance systems. In: *IEEE intelligent transportation systems conference*, Toronto, Canada, 17–20 September 2006, pp. 968–975. New York: IEEE.
30. Kaisy AA, Asce M, Bhatt J and Rakha H. Modeling the effect of heavy vehicles on sign occlusion at multilane highways. *J Transpn Engng* 2005; 131: 219–228.
31. Ioannou P and Xu Z. Throttle and brake control systems for automatic vehicle following. California PATH Program Research Paper UCB-ITS-PRR-94-10, Institute of Transportation Studies, University of California, Berkeley, California, USA, 1994.
32. Mohan D, Tsimhoni O, Sivak M and Flannagan MJ. Road safety in India: challenges and opportunities. Report UMTRI-2009-1, Transportation Research Institute, The University of Michigan, Ann Arbor, Michigan, USA, 2009.
33. Rajaraman R, Hassan A and Padmanaban J. Analysis of road traffic accidents on NH45 (Kanchipuram District). SAE paper 2009-28-0056, 2009.
34. Ashok Leyland. Hawk 160. Technical specification, http://international.ashokleyland.com/hawk160.php (2014, accessed May 2014).

Appendix 1

Notation

a	acceleration of the vehicle (m/s^2)
a_h	acceleration of the host vehicle (m/s^2)
a_l	acceleration of the lead vehicle (m/s^2)
a_b	brake chamber area (m^2)
a_{b_f}	area of the front brake chamber (m^2)
a_{b_r}	area of the rear brake chamber (m^2)
a_f	frontal area of the vehicle (m^2)
a_1	constant
a_2	constant
c_d	aerodynamic drag coefficient
f_r	coefficient of rolling resistance
F_{bf}	braking force developed at each of the front tyres (N)
F_{br}	braking force developed at each of the rear tyres (N)
F_{fpl}	spring pre-load in the front brake chamber (N)
F_{rpl}	spring pre-load in the rear brake chamber (N)
h	headway time (s)
H	height of the vehicle's centre of gravity from the ground level (m)
K_{bf}	proportion of the total braking force on the front wheels
K_{br}	proportion of the total braking force on the rear wheels
l_{sa}	length of the slack adjuster (m)
L	length of the wheelbase (m)
L_1	distance from the vehicle's centre of gravity to the front axle (m)
L_2	distance from the vehicle's centre of gravity to the rear axle (m)
M	mass of the vehicle (kg)
p_{atm}	atmospheric pressure (N/m^2)
p_b	pressure in the brake chamber (N/m^2)
p_{co}	contact pressure of the brake chamber (N/m^2)
r_c	effective radius of the S-cam (m)
r_d	inner radius of the brake drum (m)
r_t	radius of the tyre (m)
R_a	aerodynamic resistance (N)
R_g	grade resistance (N)
R_r	total rolling resistance (N)
R_{rf}	rolling resistance of each of the front tyres (N)
R_{rr}	rolling resistance of each of the rear tyres (N)
s_o	headway offset (m)

v	velocity of the vehicle (m/s)
v_h	velocity of the host vehicle (m/s)
v_l	velocity of the lead vehicle (m/s)
v_r	relative velocity between the lead vehicle and the host vehicle (m/s)
W	weight of the vehicle (N)
W_f	load on each of the front wheels (N)
W_r	load on each of the rear wheels (N)
V_{reg}	input voltage to the electro-pneumatic regulator (V)
x_l	position of the lead vehicle (m)
x_h	position of the host vehicle (m)
x_r	distance between the lead vehicle and the host vehicle (m)
α	grade angle (deg)
δ	difference between the measured distance and the desired distance
η	efficiency of the brake system
μ	coefficient of adhesion at the tyre–road interface
ρ	density of air (kg/m^3)
τ	brake time delay (s)

Abbreviation

BF	brake factor